Crystal Formation Unraveled

August 28, 2020 · salve-project.de/newspress/crystal-formation-unraveled.html

August 28, 2020 – How does a crystal begin? Researchers from Ulm, Nottingham, Leeds and AIST in Japan filmed iron, gold and rhenium atoms inside carbon nanotubes as they formed crystal nuclei, atom by atom. In all three metals, the atoms first gathered into a disordered cluster that only later turned crystalline, the long-debated two-step path of nucleation.

Every crystal starts as a handful of atoms that, at some moment, fall into order. That moment decides the structure and size of the crystals that follow, and with them the properties of materials from semiconductors to drugs. Yet it had never been watched atom by atom. Researchers from Ulm University, the Universities of Nottingham and Leeds and the National Institute of Advanced Industrial Science and Technology (AIST) in Japan have now filmed the birth of metal crystals inside carbon nanotubes, with every atom visible.

The team of Kecheng Cao, Johannes Biskupek, Andrei Khlobystov and Ute Kaiser followed three metals: iron, gold and rhenium. Each found its own way to the crystal, but all three took the same detour. The atoms first gathered into a disordered, amorphous cluster, and only this cluster turned into a crystal. Such a two-step path had been postulated in theory and debated for years. The images now show it directly.

One step or two?

The classical nucleation theory describes crystal formation in a single step: atoms, ions or molecules attach one by one to an ordered structure until it is large enough to grow on its own (Fig. 1a)[1],[2]. Many observations do not fit this picture, and so a two-step nucleation mechanism was proposed (Fig. 1b)[3]–[5]. In it, an amorphous precursor forms first and is replaced by a crystalline phase only in a second step[6]–[8]. The precursor may also have to reach a certain size before it can crystallize, as sketched in Fig. 1c[9],[10].

Testing these ideas is hard because the decisive stage is small and fast. Cryogenic electron microscopy freezes nucleation at discrete moments[11],[12], and X-ray diffraction[13], atomic force microscopy[1],[14] and optical microscopy[15] are too slow or too coarse for single atoms. Liquid-cell electron microscopy can follow the growth of metal nanocrystals in solution in real time, but the liquid and the cell windows scatter the electrons, and the very first steps stay out of sight. Critical nuclei are thought to contain 100 to 1000 atoms, a size no method could resolve atom by atom, so a conceptually new approach was needed[16].

Test tubes, an atomic injector and an electron beam

The team used single-walled carbon nanotubes (SWNTs) as test tubes only about 1.5 nm wide[17]–[19]. The tubes are transparent to electrons, chemically and thermally stable, and their wall serves as a substrate on which a crystal nucleus can form. Inside the tube, the metal atoms cannot escape, and they stay in the field of view of the microscope.

The nanotubes were filled with vapors of metal compounds, which left metal atoms and small clusters inside (recipe in the box). In Ulm, the samples were imaged with an aberration-corrected FEI Titan 80-300 microscope at 80 kV (AC-HRTEM), in time series of up to several minutes. At 80 kV the electrons do not knock carbon atoms out of the tube wall. The electron beam does two jobs at once: it takes the pictures and it transfers small amounts of energy to the metal atoms, much like heating. This energy drives the nucleation.

For iron, the team found an unexpected helper. Ferrocene, the iron compound used for filling, leaves behind mobile clusters of amorphous carbon that carry iron atoms (Fig. 2). These complexes slide along the tube within seconds, because the inner wall of a nanotube is almost frictionless. Electron energy loss maps recorded at AIST with a scanning transmission electron microscope (STEM) at 60 kV confirmed the iron in them. The team called them “atomic injectors”: they deliver iron atoms, one by one, to a growing nucleus.

Recipe: metals into nanotubes

Nanotubes made by arc discharge were heated in air to open their ends. Each was then sealed under vacuum in a quartz ampoule together with one metal compound: ferrocene, $Fe(C_5H_5)_2$, gold carbonyl chloride, Au(CO)Cl, or dirhenium decacarbonyl, $Re_2(CO)_{10}$. The ampoules were kept for three days just above the temperature at which the compound evaporates (300 °C for ferrocene, 125 °C for Au(CO)Cl and 150 °C for $Re_2(CO)_{10}$), so the vapor entered the tubes.

After rapid cooling, the tubes were washed with tetrahydrofuran to remove everything on the outside and heated to 500 °C for 3 hours under argon, which removed the ligands and left the metal inside. For microscopy, the material was dispersed in methanol, dropped onto lacey carbon TEM grids and heated in air at 150 °C for 5 min just before it went into the microscope.

The time series were recorded on the image-side corrected FEI Titan 80-300 in Ulm at 80 kV and room temperature. The STEM images and EELS maps in Fig. 2 were taken on a JEOL 2100F with a cold field-emission gun and a DELTA corrector at 60 kV. Image simulations were done with the multislice program QSTEM.

Iron: from two atoms to a crystal in four stages

The full birth of an iron crystal was recorded in one experiment at a dose rate of 1.4×10^6 electrons per nm^2 and second (Video 1). It ran through four stages (Fig. 3 and 4).

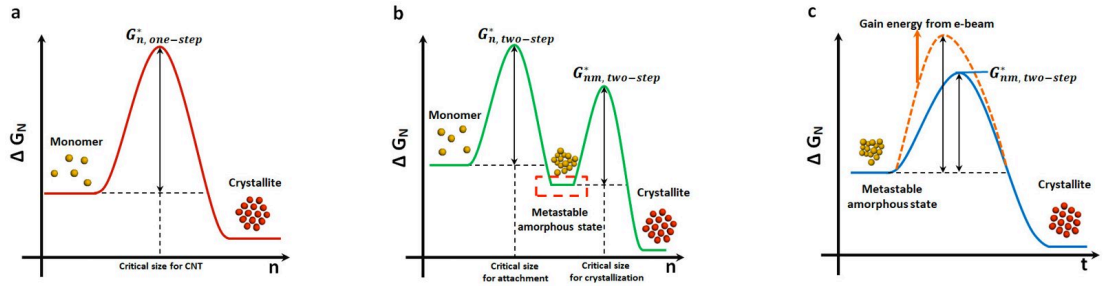

Fig. 1: Free energy: one-step versus two-step nucleation.

Diatomic seed (0–13 s): Two iron atoms form a pair on the outside of the tube wall, 0.32 to 0.34 nm apart (Fig. 3). A free Fe_2 molecule would have a bond length of only 0.20 nm. The tube stretches the pair to a distance much closer to that in bulk γ-iron (0.29 nm), and in doing so it weakens the bond from 2.2 eV to 0.8 eV. At 8 s, the right iron atom passes through the wall into the tube, which points to a vacancy defect in the wall at this spot.

Atom delivery (13–50 s): An atomic injector slides along the tube towards the seed and pushes its right atom aside, to 0.43 nm (Fig. 3a–c). This frees space, and at 19 s a third atom moves from the injector into the seed. Within the next 4 s the seed grows into a cluster of about 17 iron atoms, while only one atom remains in the injector. The cluster stays amorphous. Once it has handed over its atoms, the injector moves on along the tube.

Metastable amorphous state (50–197 s): For 147 s the cluster keeps rearranging. Its atoms shuttle between the inner and outer surface of the tube, and their distances and neighbors change all the time (Fig. 4a).

Ordered crystallite (from 197 s): Suddenly the atoms line up at equal distances that match the (111) plane of γ-iron. From now on, further growth follows this ordered core. Fourier transforms of the images measure how the order appears over time (Fig. 4b, c).

The amorphous stage is the key result. A pair of iron atoms can still fall apart again, and clusters of about 10 atoms neither fall apart nor crystallize. The 17-atom cluster, in contrast, stayed amorphous for more than 142 s before it ordered. A metastable amorphous precursor is therefore necessary for iron to nucleate, and the process follows the two-step mechanism[8], as detailed in the box.

Iron: how many atoms make a crystal

Density functional theory calculations by the Nottingham team give the energy needed to split iron clusters into single atoms: 2.2 eV for Fe_2 (1.1 eV per atom) and 4.3 eV for Fe_3 (1.4 eV per atom). Stretching the dimer to 0.43 nm, as the injector did, lowers its binding energy by 90 % to only 0.2 eV, so the two atoms are held apart by the tube rather than by each other.

In further time series, an iron pair on the tube wall came loose and split apart under the beam within about a minute. Clusters with fewer than 10 iron atoms stayed amorphous for more than 240 s without falling apart or crystallizing. A γ-iron crystallite of about 100 atoms, on the other hand, kept its order under the beam. So, under these conditions, more than 10 iron atoms are necessary and 17 are sufficient for a crystal nucleus. The exact number may change with the conditions, since the electron beam is known to affect nucleation[20],[21].

The 17 atoms were counted by image simulation. The tube was identified as an (18,2) nanotube from its diameter of about 1.5 nm and its Fourier transform. A single iron atom and two atoms stacked along the beam give clearly different contrast, and a simulated crystallite of 17 atoms matches the measured intensities, while the largest one that fits into the tube, 27 atoms, would look too dark.

Under continued irradiation, the finished γ-iron crystallite started to remove carbon atoms from the tube. A vacancy defect grew until the tube was cut through after 170 s[17]. Neither the iron pair nor the amorphous cluster had attacked the tube like this, so the crystal is chemically more active than its disordered precursor.

Gold: order inside an amorphous cluster

For gold, the starting point was a larger amorphous cluster already sitting in the tube (Fig. 5). Some of its atoms diffused into a neighboring carbon structure (violet arrow in Fig. 5a). For the first 16 s under the beam, the cluster was extremely dynamic and showed no order. At 17 s, a crystallite less than 1 nm across appeared inside it, confirmed by its Fourier transform (Fig. 5b). It dissolved within 5 s and reappeared at 23 s.

Once it reached about 1 nm, it stayed, with a well-ordered (111) face of gold. From there, the order spread through the whole cluster over the next 348 s, until the crystallite was about 2 nm long and 1 nm wide at 370 s. In between, it rotated or transformed and showed other orientations, and from 331 s on it returned to the original (111) face. The intensity of the gold reflections in the Fourier transforms jumps when the cluster crystallizes (Fig. 5c), so gold, too, forms its crystal out of an amorphous precursor (Fig. 5d).

The energy for this step comes from the beam. An 80 keV electron can transfer at most 0.96 eV to a gold atom. Earlier work had shown that such energy transfer can affect, melt and even evaporate metal nanocrystals[22]. Here it was just enough for the cluster to overcome the barrier between the amorphous and the crystalline state. The smallest gold crystallite seen had a radius of only about 0.45 nm, much smaller than the 2 nm nuclei observed for gold in the solution of a liquid cell[20].

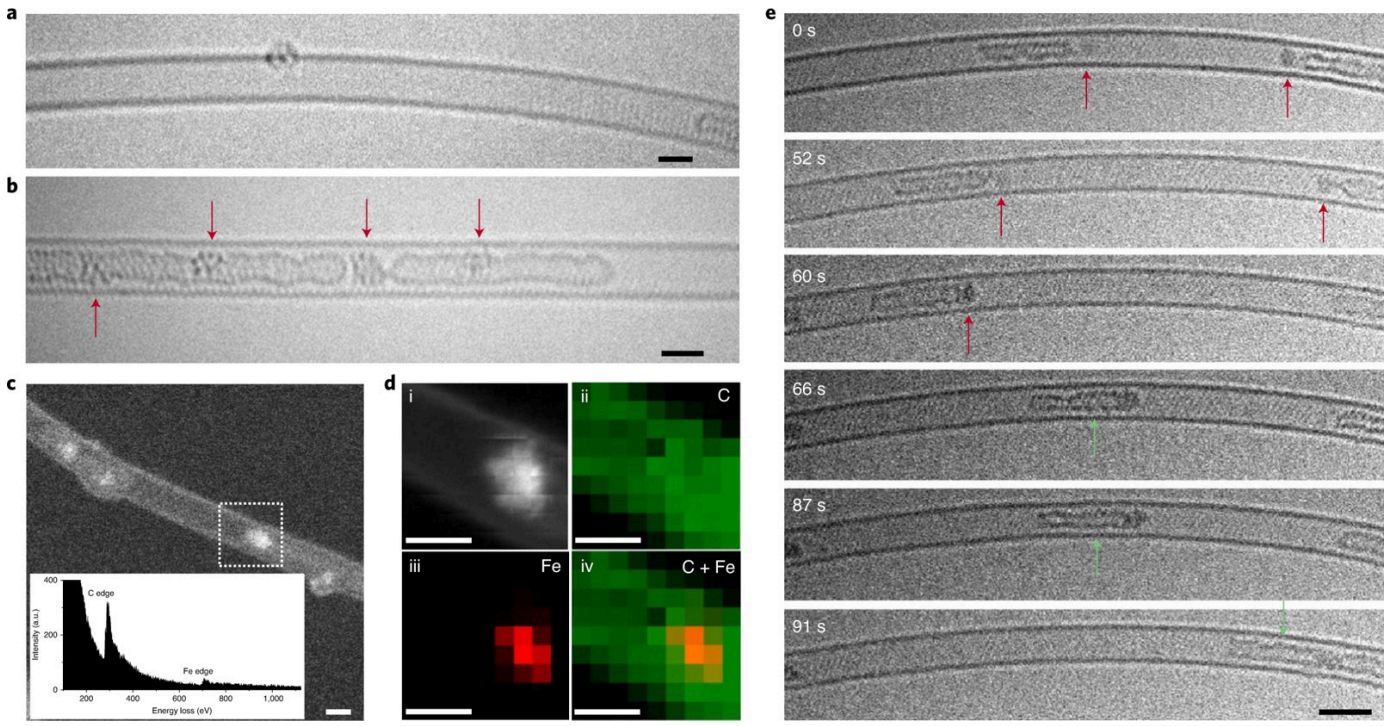

Fig. 2: Fe@SWNT: HRTEM, STEM-EELS and atomic injector.

Rhenium: two clusters merge

More atoms make it easier to overcome the energy barrier, so clusters that merge can speed up nucleation. Classical theory usually ignores this route. With rhenium, the team watched it happen (Fig. 6). At the start, two amorphous rhenium clusters of about 10 atoms each sat in the tube. The left one was mobile and moved along the tube. The right one was bound to the wall and partly covered by a carbon shell, which served as the substrate for nucleation.

At 135 s, the left cluster attached to the carbon shell of the right one. At 151 s and 177 s, the two touched briefly through a single rhenium atom, and between 183 s and 185 s they merged completely. The new cluster of about 20 atoms was above the critical size. It stayed amorphous at first and reorganized until, at 308 s, a crystallite with clear lattice planes appeared. For another 124 s it kept restructuring while remaining crystalline (Fig. 6b, c). Rhenium thus follows the same two-step path as iron and gold, except that it reaches the critical size by coalescence.

What it opens up

All three metals crystallized through a metastable amorphous precursor, at room temperature and under the electron beam. The size of this precursor decides whether a crystal forms: for all three metals the critical size is below 2 nm, and for iron and rhenium it lies between 10 and 20 atoms. What differed was how the cluster got there: by collecting single atoms (iron), by ordering an existing amorphous cluster (gold) or by the coalescence of two small clusters (rhenium).

The combination of a nanotube as substrate and delivery channel, and the electron beam as both energy source and camera, opens up a size range below one nanometer that no other method reaches. The results matter for iron, gold and rhenium in carbon-rich environments found in industry, such as Fischer–Tropsch catalysis, the growth of graphene by chemical vapor deposition and steelmaking. Ute Kaiser said: “By successfully recording this process, we hope that in action we will shed light on the fundamental phenomenon of nucleation and crystal growth for the three metals examined and enable a more controlled design of materials in the future.”

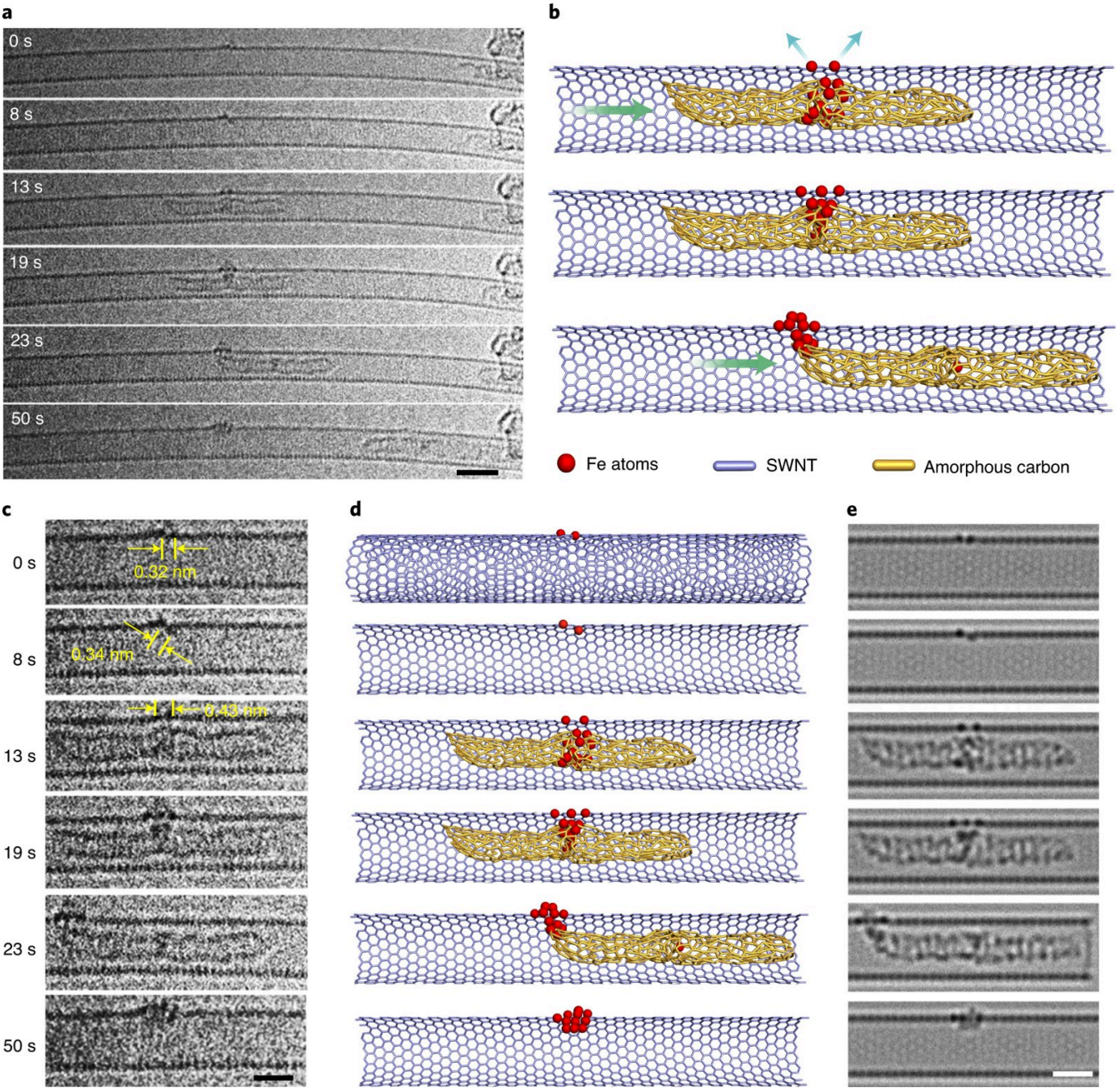

Fig. 3: Iron, stages 1–2: seed and atom delivery.

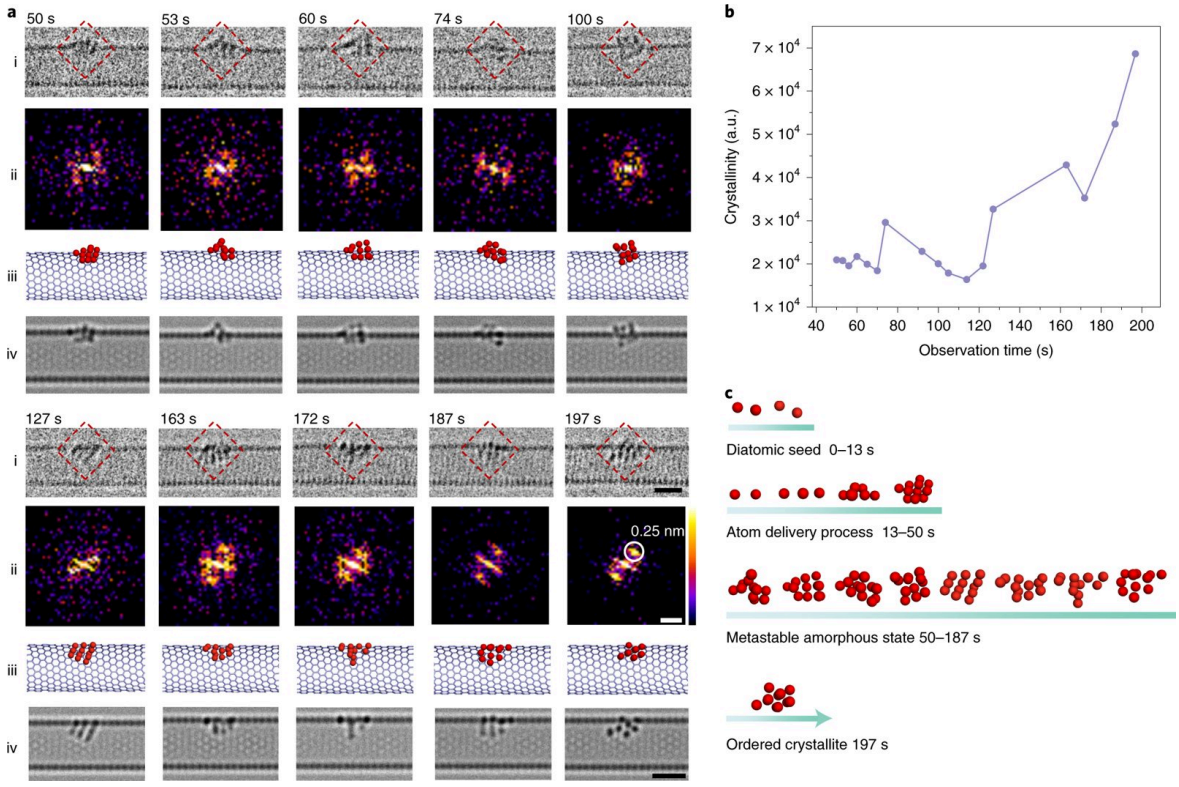

Fig. 4: Iron, stages 3–4: amorphous, then crystalline.

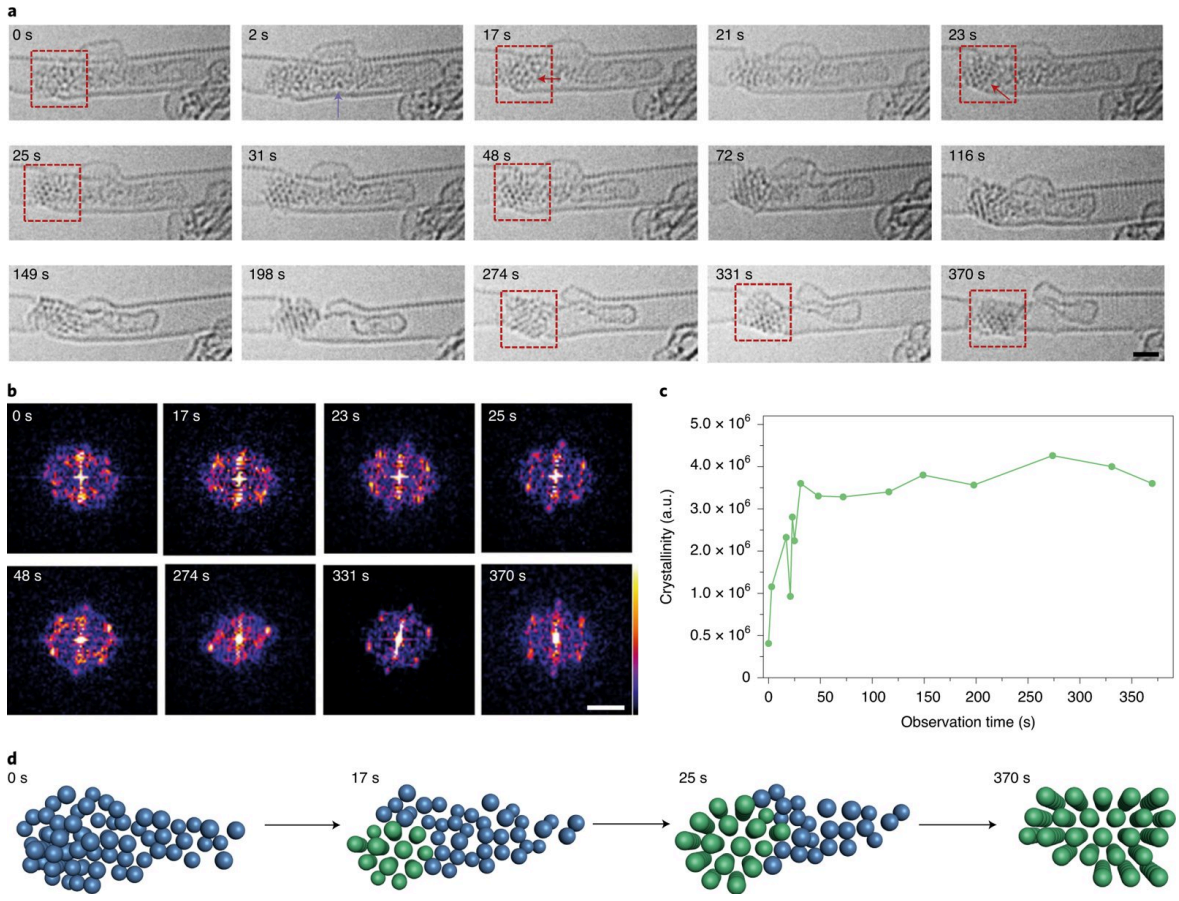

Fig. 5: Gold: crystallite grows inside amorphous cluster.

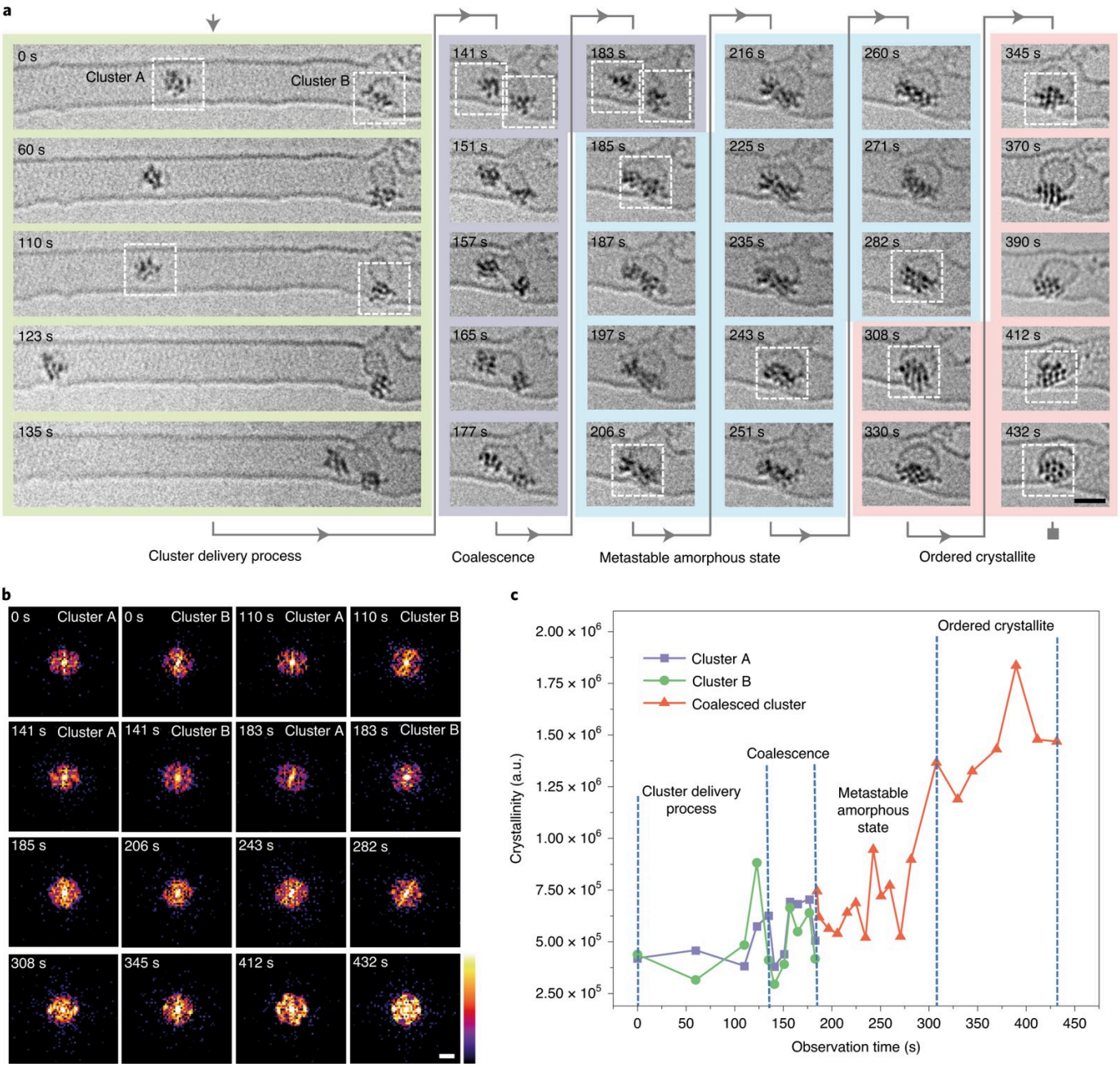

Fig. 6: Rhenium: two clusters merge, then crystallize.

Resource

Cao, K., Biskupek, J., Stoppiello, C. T., McSweeney, R. L., Chamberlain, T. W., Liu, Z., Suenaga, K., Skowron, S. T., Besley, E., Khlobystov, A. N., Kaiser, U. (2020). Atomic mechanism of metal crystal nucleus formation in a single-walled carbon nanotube.
Nat. Chem. **12**(10), 921–928.
https://doi.org/10.1038/s41557-020-0538-9

References

1. Sleutel, M., Lutsko, J., Van Driessche, A., Durán-Olivencia, M., Maes, D. (2014). Observing Classical Nucleation Theory at Work by Monitoring Phase Transitions With Molecular Precision. *Nat. Commun.*, **5**, 5598. https://doi.org/10.1038/ncomms6598
2. Habraken, W., Tao, J., Brylka, L., Friedrich, H., Bertinetti, L., Schenk, A., Verch, A., Dmitrovic, V., Bomans, P., Frederik, P., Laven, J., van der Schoot, P., Aichmayer, B., de With, G., DeYoreo, J., Sommerdijk, N. (2013). Ion-Association Complexes Unite Classical and Non-Classical Theories for the Biomimetic Nucleation of Calcium Phosphate. *Nat. Commun.*, **4**, 1507. https://doi.org/10.1038/ncomms2490
3. Dey, A., Bomans, P., Müller, F., Will, J., Frederik, P., de With, G., Sommerdijk, N. (2010). The Role of Prenucleation Clusters in Surface-Induced Calcium Phosphate Crystallization. *Nat. Mater.*, **9**, 1010–1014. https://doi.org/10.1038/nmat2900
4. Erdemir, D., Lee, A., Myerson, A. (2009). Nucleation of Crystals From Solution: Classical and Two-Step Models. *Acc. Chem. Res.*, **42**, 621–629. https://doi.org/10.1021/ar800217x
5. Gebauer, D., Cölfen, H. (2011). Prenucleation Clusters and Non-Classical Nucleation. *Nano Today*, **6**, 564–584. https://doi.org/10.1016/j.nantod.2011.10.005

6. Nielsen, M., Aloni, S., De Yoreo, J. (2014). In Situ TEM Imaging of $CaCO_3$nucleation Reveals Coexistence of Direct and Indirect Pathways. *Science*, **345**, 1158–1162. https://doi.org/10.1126/science.1254051
7. Gal, A., Habraken, W., Gur, D., Fratzl, P., Weiner, S., Addadi, L. (2013). Calcite Crystal Growth by a Solid-State Transformation of Stabilized Amorphous Calcium Carbonate Nanospheres in a Hydrogel. *Angew. Chem. Int. Ed.*, **52**, 4867–4870. https://doi.org/10.1002/anie.201210329
8. Navrotsky, A. (2004). Energetic Clues to Pathways to Biomineralization: Precursors, Clusters, and Nanoparticles. *Proc. Natl. Acad. Sci. USA*, **101**, 12096–12101. https://doi.org/10.1073/pnas.0404778101
9. Wolf, S., Leiterer, J., Kappl, M., Emmerling, F., Tremel, W. (2008). Early Homogenous Amorphous Precursor Stages of Calcium Carbonate and Subsequent Crystal Growth in Levitated Droplets. *J. Am. Chem. Soc.*, **130**, 12342–12347. https://doi.org/10.1021/ja800984y
10. Gebauer, D., Völkel, A., Cölfen, H. (2008). Stable Prenucleation Calcium Carbonate Clusters. *Science*, **322**, 1819–1822. https://doi.org/10.1126/science.1164271
11. Baumgartner, J., Dey, A., Bomans, P., Le Coadou, C., Fratzl, P., Sommerdijk, N., Faivre, D. (2013). Nucleation and Growth of Magnetite From Solution. *Nat. Mater.*, **12**, 310–314. https://doi.org/10.1038/nmat3558
12. Tsarfati, Y., Rosenne, S., Weissman, H., Shimon, L., Gur, D., Palmer, B., Rybtchinski, B. (2018). Crystallization of Organic Molecules: Nonclassical Mechanism Revealed by Direct Imaging. *ACS Cent. Sci.*, **4**, 1031–1036. https://doi.org/10.1021/acscentsci.8b00289
13. Bera, M., Antonio, M. (2016). Crystallization of Keggin Heteropolyanions via a Two-Step Process in Aqueous Solutions. *J. Am. Chem. Soc.*, **138**, 7282–7288. https://doi.org/10.1021/jacs.5b13375
14. Lupulescu, A., Rimer, J. (2014). In Situ Imaging of Silicalite-1 Surface Growth Reveals the Mechanism of Crystallization. *Science*, **344**, 729–732. https://doi.org/10.1126/science.1250984
15. Pusey, P., van Megen, W. (1986). Phase Behaviour of Concentrated Suspensions of Nearly Hard Colloidal Spheres. *Nature*, **320**, 340–342. https://doi.org/10.1038/320340a0
16. Sosso, G., Chen, J., Cox, S., Fitzner, M., Pedevilla, P., Zen, A., Michaelides, A. (2016). Crystal Nucleation in Liquids: Open Questions and Future Challenges in Molecular Dynamics Simulations. *Chem. Rev.*, **116**, 7078–7116. https://doi.org/10.1021/acs.chemrev.5b00744
17. Cao, K., Zoberbier, T., Biskupek, J., Botos, A., McSweeney, R., Kurtoglu, A., Stoppiello, C., Markevich, A., Besley, E., Chamberlain, T., Kaiser, U., Khlobystov, A. (2018). Comparison of Atomic Scale Dynamics for the Middle and Late Transition Metal Nanocatalysts. *Nat. Commun.*, **9**, 3382. https://doi.org/10.1038/s41467-018-05831-z
18. Khlobystov, A. (2011). Carbon Nanotubes: From Nano Test Tube to Nano-Reactor. *ACS Nano*, **5**, 9306–9312. https://doi.org/10.1021/nn204596p
19. Zoberbier, T., Chamberlain, T., Biskupek, J., Kuganathan, N., Eyhusen, S., Bichoutskaia, E., Kaiser, U., Khlobystov, A. (2012). Interactions and Reactions of Transition Metal Clusters With the Interior of Single-Walled Carbon Nanotubes Imaged at the Atomic Scale. *J. Am. Chem. Soc.*, **134**, 3073–3079. https://doi.org/10.1021/ja208746z
20. Loh, N., Sen, S., Bosman, M., Tan, S., Zhong, J., Nijhuis, C., Král, P., Matsudaira, P., Mirsaidov, U. (2017). Multistep Nucleation of Nanocrystals in Aqueous Solution. *Nat. Chem.*, **9**, 77–82. https://doi.org/10.1038/nchem.2618
21. Zheng, H., Smith, R., Jun, Y., Kisielowski, C., Dahmen, U., Alivisatos, A. (2009). Observation of Single Colloidal Platinum Nanocrystal Growth Trajectories. *Science*, **324**, 1309–1312. https://doi.org/10.1126/science.1172104
22. Skowron, S., Chamberlain, T., Biskupek, J., Kaiser, U., Besley, E., Khlobystov, A. (2017). Chemical Reactions of Molecules Promoted and Simultaneously Imaged by the Electron Beam in Transmission Electron Microscopy. *Acc. Chem. Res.*, **50**, 1797–1807. https://doi.org/10.1021/acs.accounts.7b00078